Appendix A: Supplementary Materials

This document contains some detailed figures to support the results presented in the main paper, including

- Fig. 6, measured ZLE efficiency vs. $S1$ using the LED calibration run;
- Fig. 7, the evolution of electron lifetime during Run 9 and Run 10;
- Fig. 8, the fits to ER peaks and the energy resolution vs. energy;
- Fig. 9, the best fits and 1σ contour for the PDE and EEE parameter scans;
- Fig. 10, vertical distribution for single scatter NR events from AmBe calibration run and the de-composition of real single scatter and "neutron-X" events;
- Fig. 11 Measurement of double PE emission rate using LXe data
- Fig. 12, data and MC comparison for AmBe NR events;
- Fig. 13, data and MC comparison for $E_{\rm comb}$ spectrum as well as light and charge yields for tritium β-decay events;
- Fig. 14, data and MC comparison of $\log_{10}(S2/S1)$ in different $S1$ slices for tritium β-decay events;
- Fig. 15, drift time vs. reconstructed radius for the wall ^{210}Po events, Run 9 and Run 10;
- Fig. 16, detection efficiency vs. NR recoil energy and WIMP mass
- Fig. 17, energy spectra of the measured and best fit background components below 50 keV$_{ee}$ and in the final selection window in Run 10;
- Fig. 18, exclusion curves with linear scale in WIMP mass.

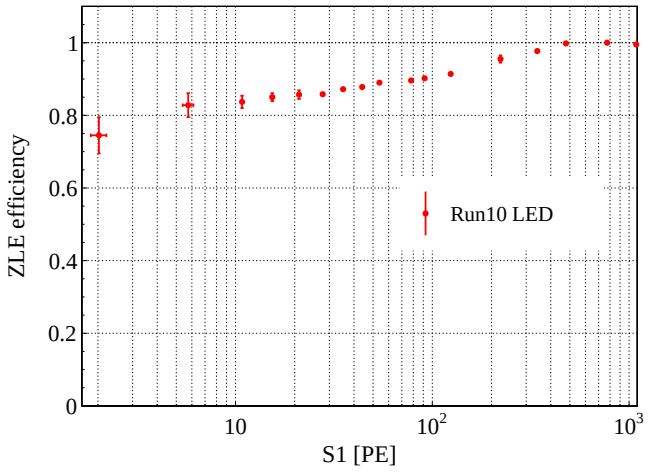

FIG. 6: The ZLE efficiency, defined as the ratio of the average $S1$ with and without ZLE, vs. $S1$ (without ZLE), measured from the LED data in Run 10. Note that the photons from the blue LED would not produce double PE emission on R11410-20 PMTs.

[1] A. Tan *et al.* (PandaX-II), Phys. Rev. Lett. **117**, 121303 (2016), arXiv:1607.07400 [hep-ex].
[2] D. S. Akerib *et al.* (LUX), Phys. Rev. Lett. **118**, 021303 (2017), arXiv:1608.07648 [astro-ph.CO].
[3] E. Aprile *et al.* (XENON), (2017), arXiv:1705.06655 [astro-ph.CO].
[4] X. Ji, in *TeV Particle Astrophysics 2017* (Columbus, Ohio, US, 2017) `https://tevpa2017.osu.edu/talks/ji.pdf`.

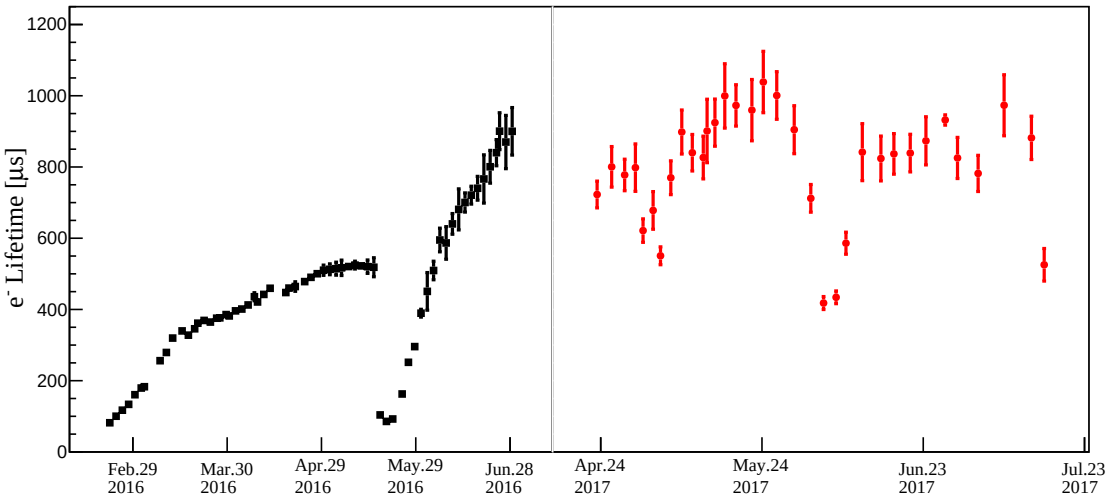

FIG. 7: Evolution of the electron lifetime in Run 9 (left) and Run 10 (right). Each point represent the average in a data taking unit, usually lasted for a few days. Data with electron lifetime longer than 205 μs were used in the dark matter analysis.

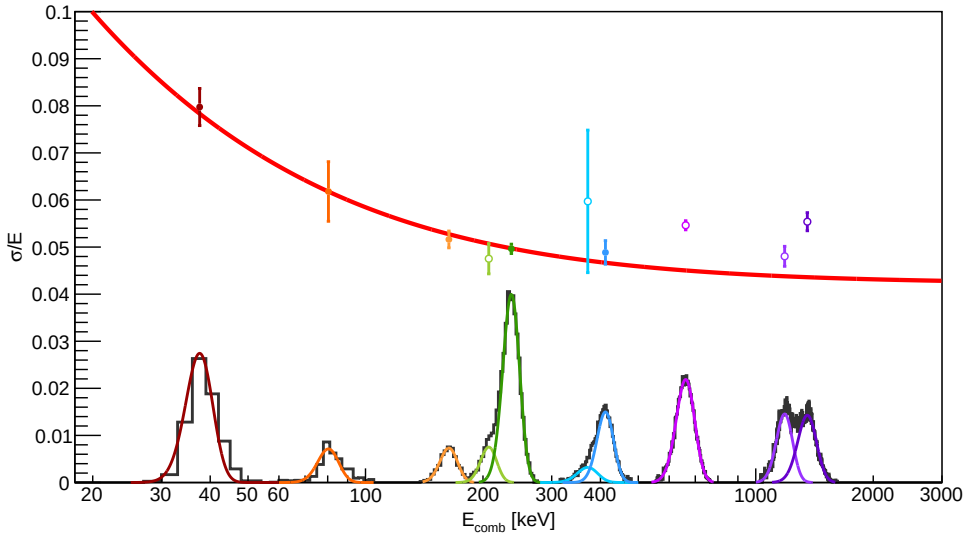

FIG. 8: Energy resolution vs. E_{comb} in Run 10 overlaid with the ER peaks in the data: 39.6 keV (n, ^{129}Xe*), 80.2 keV (n, ^{131}Xe*), 164 keV (^{131m}Xe), 236 keV (^{129m}Xe), 203, 375, and 408 keV (^{127}Xe), 662 keV (^{137}Cs), and 1173 and 1332 keV (^{60}Co). Spectra are scaled for visual clarity, and fitted with multiple Gaussians. The data points represent the energy resolution correponding to the fitted Gaussians with the same color. Solid red line represents the fit in the form of $\sigma/E = \sqrt{p_0/E + p_1}$. Open circles were not included in the fit.

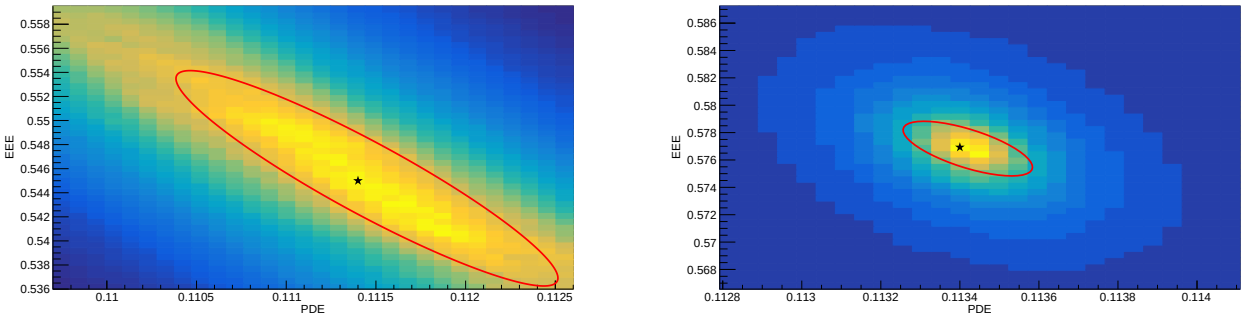

(a)Run 9 (b)Run 10

FIG. 9: The PDE and EEE combined scan (left: Run 9, right: Run 10) with $1/\chi^2$ as the weight. The χ^2 is defined as $\sum_i (E^i_{\text{comb}} - E^i_{\text{expect}})^2/(\delta E^i_{\text{comb}})^2$ where i loops over all fitted ER peaks and δE^i_{comb} is the corresponding peak uncertainty. The black stars represent the best fits and red ellipses correpond to the 1σ contours used to determine the uncertainties.

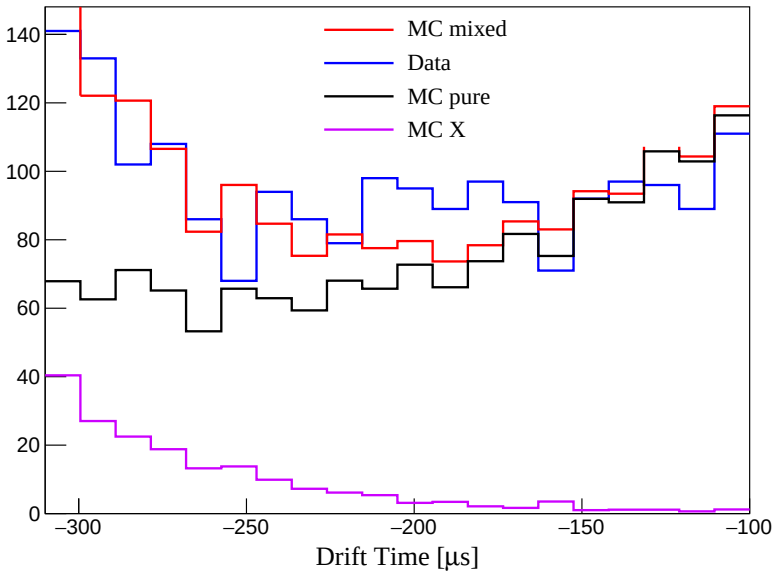

FIG. 10: The vertical distribution of the AmBe NR events (blue), overlaid with pure single scatter NR (black), "neutron-X" (magenta), and the total mixed events (red) from the MC.

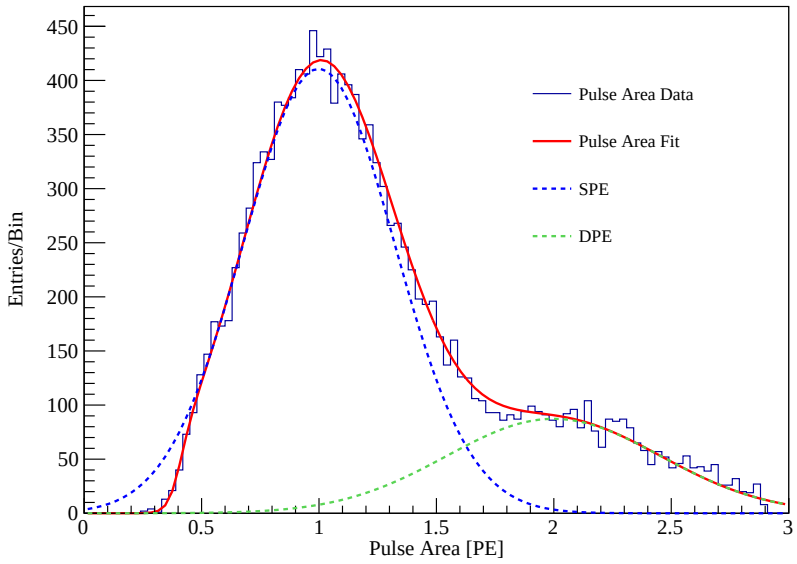

FIG. 11: Measured waveform area for smallest $S1$-like signal with only one fired PMT channel, in units of PE, for a representative PMT channel, fitted with a double-Gaussian folded with a Fermi-Dirac efficiency function. The probability of double PE emission was derived using number of double PE entries over total entries to be 0.22 ± 0.02.

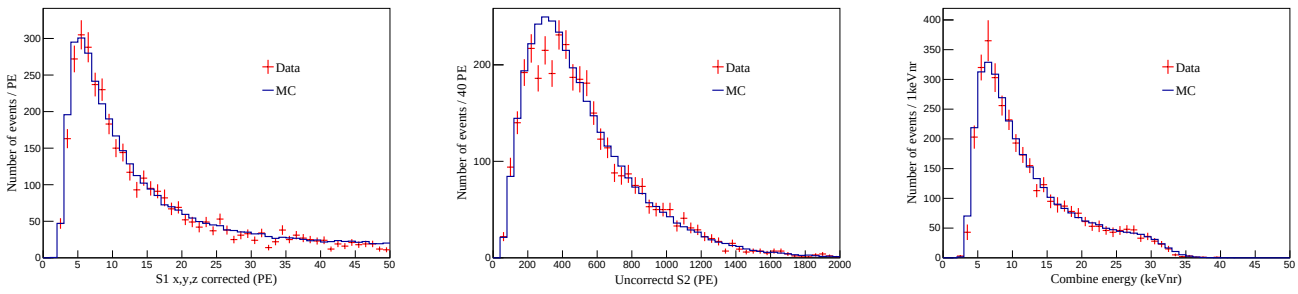

(a)$S1_{\text{corrected}}$ spectrum (b)$S2_{\text{raw}}$ spectrum (c)Energy Spectrum in keV_{nr}

FIG. 12: The comparison of $S1_{\text{corrected}}$ (a), $S2_{\text{raw}}$ (b), and combined energy spectrum in nuclear recoil energy keV_{nr}(c) between NR data and MC (efficiency considered) with tuned NEST.

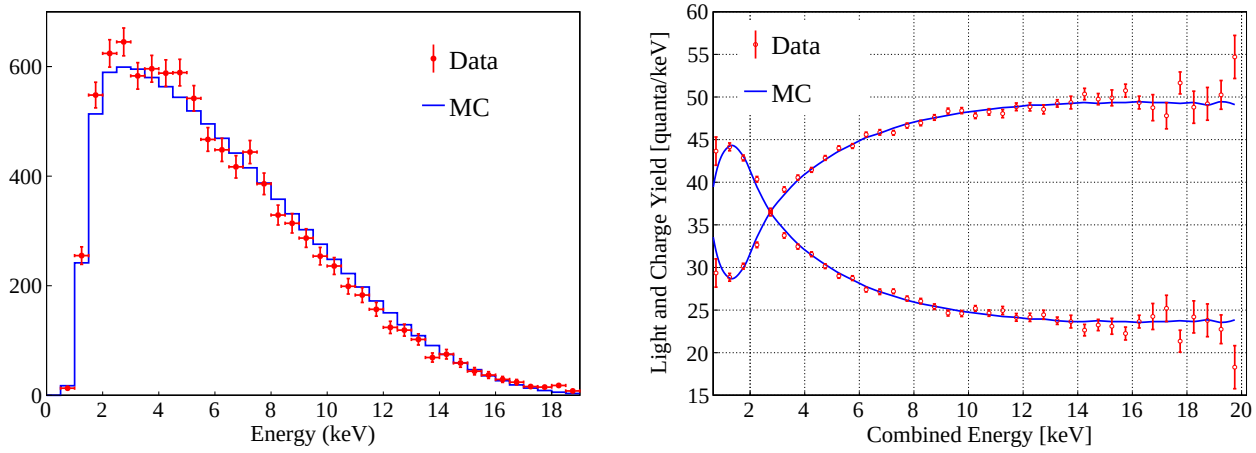

(a)tritium energy spectrum

(b)LY and CY

FIG. 13: Left: combined energy spectrum of the tritium data (red) and MC (blue); right: light yield, (LY=$S1$/PDE/E_{comb}) and charge yield (CY=$S2$/EEE/SEG/E_{comb}) vs. E_{comb} from tritium data (red circles) in Run 9 (400 V/cm drift field), in comparison to those from tuned NEST model (blue curves). The LY(CY) corresponds to the upper (lower) curve at higher energy.

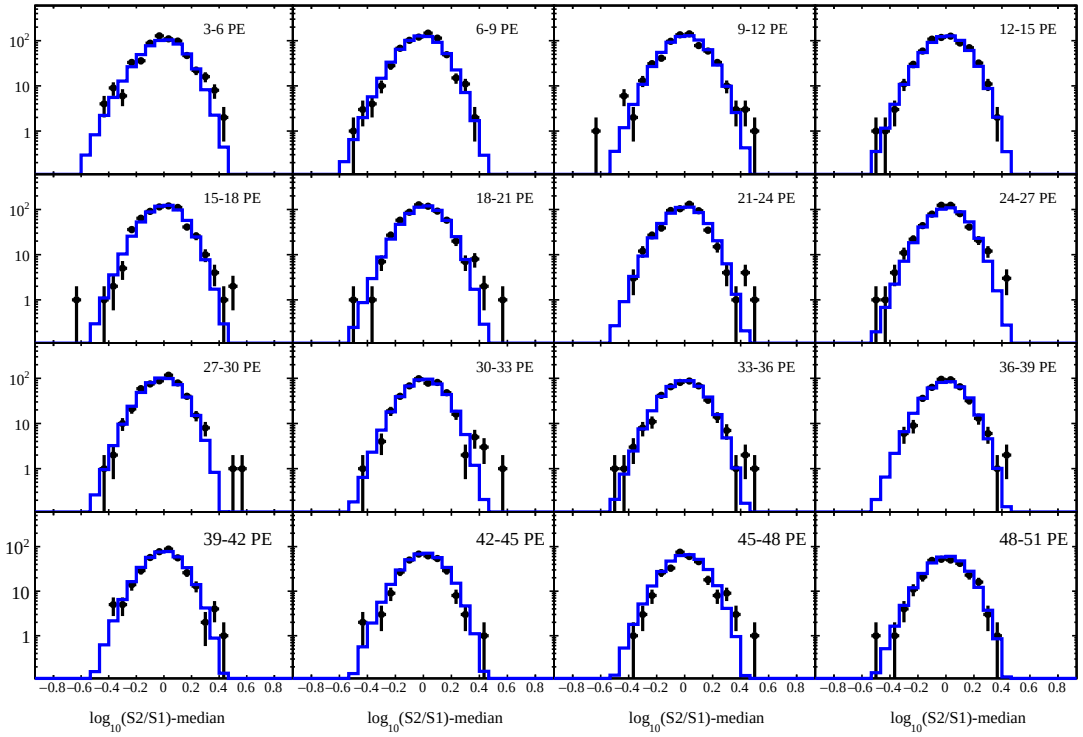

FIG. 14: Distribution of $\log_{10}(S2/S1)$ in different $S1$ slices for tritium data (black) and MC (blue).

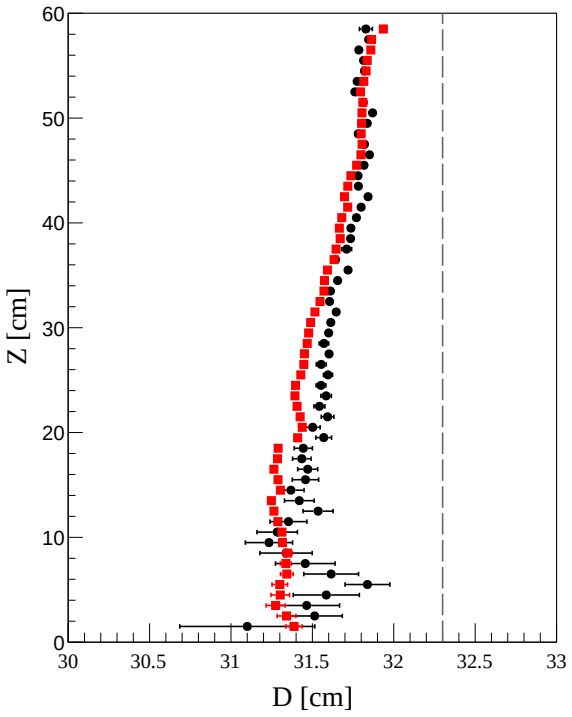

FIG. 15: The distribution of the distance with respect to PTFE panels of plated-out ^{210}Po α events in Run 9 (black circle) and Run 10 (red square). The dashed gray line indicates the PTFE panels located at D=32.3 cm. A small slant of the "wall" was observed, indicating the magnitude of the field distortion.

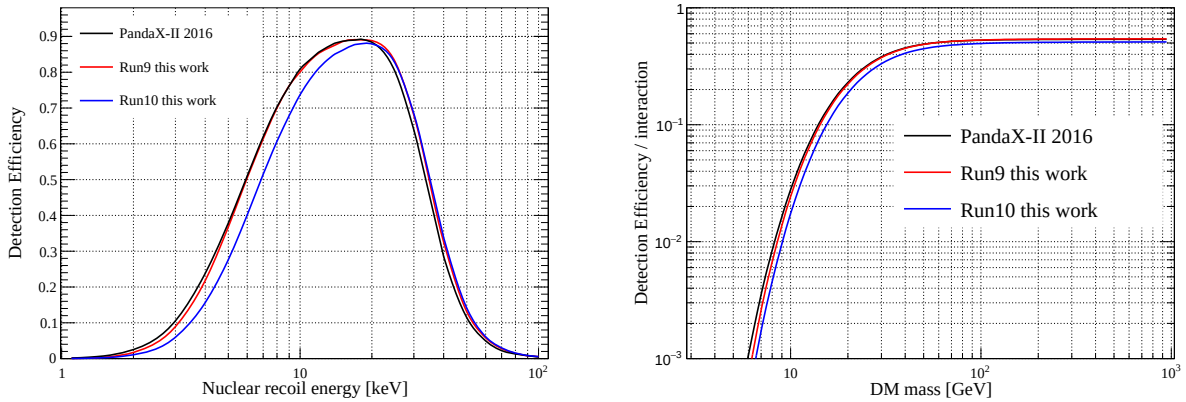

(a)ϵ vs. $E_{\rm nr}$ (b)ϵ vs. m_χ

FIG. 16: Exposure-weighted detection efficiency vs. NR energy (a) and WIMP mass (b), for Run 9 (red), Run 10 (blue), and PandaX-II 2016 (black). The difference in acceptance is due to the update of PDE and EEE in this analysis. The difference between Run 9 and Run 10 is primarily due to the ZLE effects.

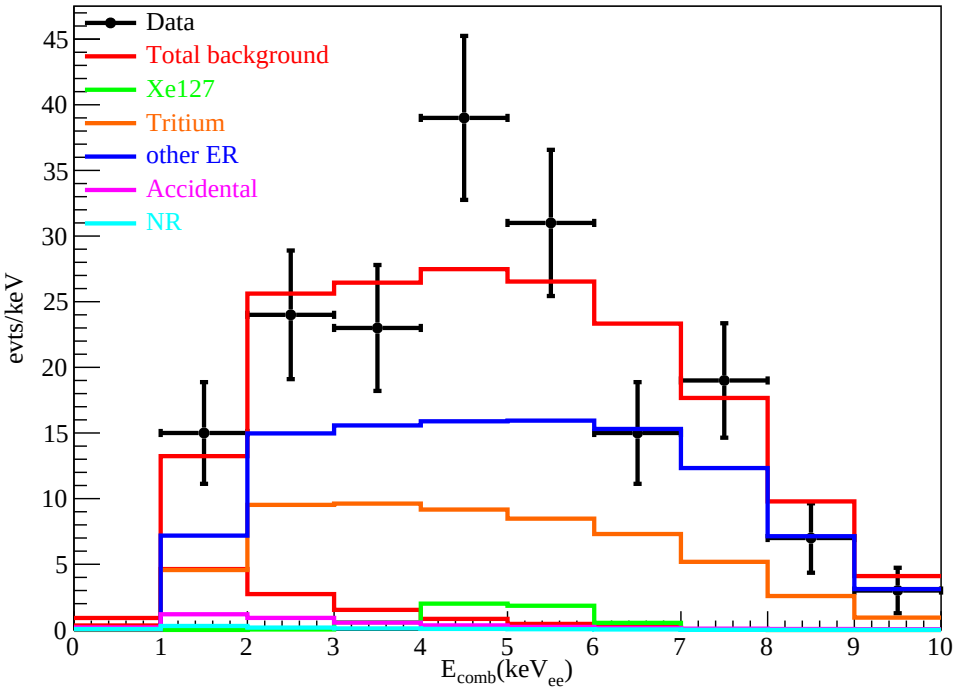

(a)final candidates in DM search window

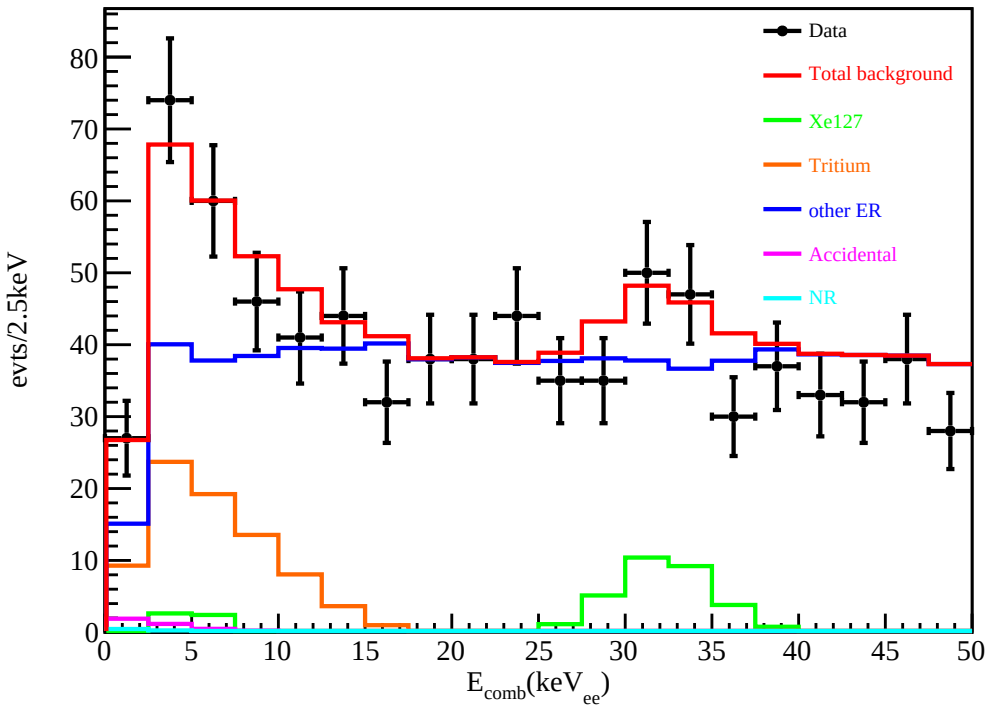

(b)0-50 keV

FIG. 17: Left: $E_{\rm comb}$ of the final candidates in Run 10 overlaid with best fit background components (see legend). Right: same figure but extending the energy window to 50 keV.

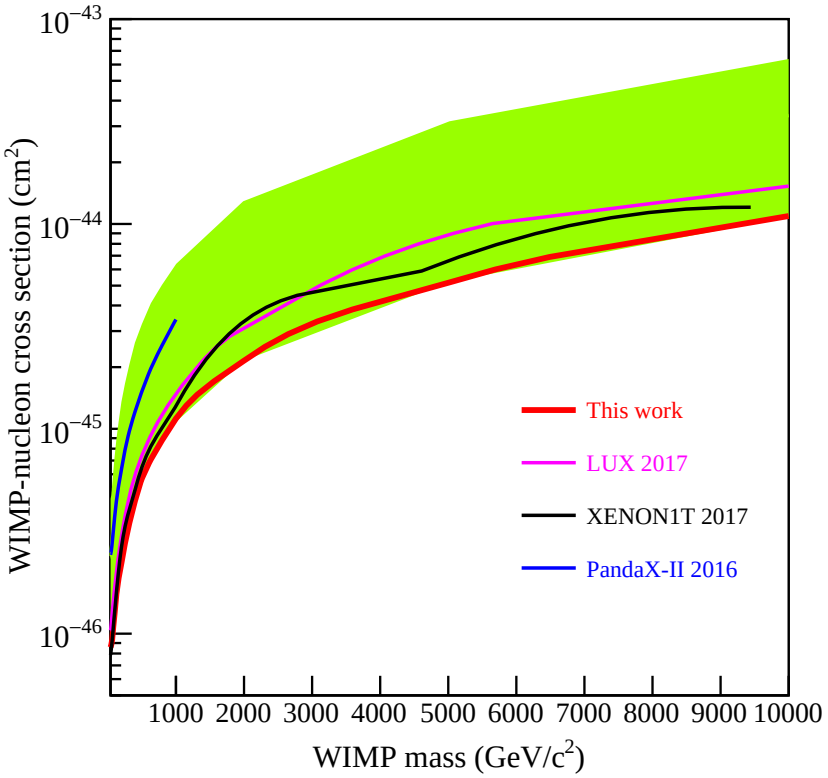

FIG. 18: The 90% C.L. upper limits for the spin independent WIMP-nucleon elastic cross sections vs. WIMP mass in linear scale between 40 GeV/c^2 to 10 TeV/c^2 from the combined PandaX-II Run 9 and Run 10 data (red, with green band as the $\pm1\sigma$ sensitivity band), overlaid with that from PandaX-II 2016 [1] (blue), LUX 2017 [2] (magenta), and XENON1T 2017 [3]. The limit presented here is more conservative than that shown at [4], which was produced using the PDE and EEE from Ref. [1]. This work contains an improved determination on PDE and EEE for both Run 9 and Run 10. The difference in EEE in different sets of data with difference gate voltages during Run 9 was also taken into account. We chose to report this more conservative limit as our final results.